TEFL: Turbo Explainable Federated Learning for 6G Trustworthy Zero-Touch Network Slicing

Swastika Roy, *Student Member, IEEE*, Hatim Chergui, *Senior Member, IEEE*
and Christos Verikoukis, *Senior Member, IEEE*

***Abstract*—Sixth-generation (6G) networks anticipate intelligently supporting a massive number of coexisting and heterogeneous slices associated with various vertical use cases. Such a context urges the adoption of artificial intelligence (AI)-driven zero-touch management and orchestration (MANO) of the end-to-end (E2E) slices under stringent service level agreements (SLAs). Specifically, the trustworthiness of the AI black-boxes in real deployment can be achieved by explainable AI (XAI) tools to build transparency between the interacting actors in the slicing ecosystem, such as tenants, infrastructure providers and operators. Inspired by the turbo principle, this paper presents a novel iterative explainable federated learning (FL) approach where a constrained resource allocation model and an *explainer* exchange—in a closed loop (CL) fashion—soft attributions of the features as well as inference predictions to achieve a transparent and SLA-aware zero-touch service management (ZSM) of 6G network slices at RAN-Edge setup under non-independent identically distributed (non-IID) datasets. In particular, we quantitatively validate the faithfulness of the explanations via the so-called attribution-based *confidence metric* that is included as a constraint in the run-time FL optimization task. In this respect, Integrated-Gradient (IG) as well as Input $\times$ Gradient and SHAP are used to generate the attributions for the turbo explainable FL (TEFL), wherefore simulation results under different methods confirm its superiority over an unconstrained Integrated-Gradient *post-hoc* FL baseline.**

***Index Terms*—6G, closed-loop, federated learning, game theory, proxy-Lagrangian, resource allocation, SLA, XAI, ZSM**

I. Introduction

6G networks are expected to effectively support a vast number of simultaneous and heterogeneous slices associated with various vertical use cases, increasing the system's complexity. For supporting such diversified services of 6G networks, over the past few years, we have glimpsed a deluge of research on AI-based autonomous management and orchestration of the end-to-end (E2E) network and services; specifically, deep learning in the telecommunication sector, including resource scheduling, resource allocation, route planning, anomaly detection [1]. In this respect, ETSI has standardized the zero-touch network and service management (ZSM) framework, where a reference architecture and AI based closed-loop management automation have been proposed [2]. It manages all operational processes and tasks expected to accomplish autonomously. On the other hand, the traditional ML schemes are cloud-centric, which becomes impractical nowadays and also unsuitable for the network slicing case because network slices are isolated, making it challenging to collect data and build centralized machine learning models. Consequently, adopting a decentralized learning approach such as Federated learning (FL) [3] is crucial to handle distributed network slices efficiently.

Despite such intelligent approaches in network automation for certain scenarios, network operators still face problems understanding how these models make decisions or exhibit certain behaviors automatically based on the knowledge they learn from network data [4]. This is due to the lack of transparency, trust, and explainability, which results from the incomprehensible nature of the black-box AI models [5]. Thus, telecommunication operators have a low interest in wide deployment in their networks because of the suspicion of facing any SLA penalty from the tenants/users for any crucial decisions [6]. This urges to look for faithful and trustworthy decisions so that it does not harm the automated network services.

Therefore, a new AI approach is required which gives understandable and explainable decisions [7]. In this respect, recently, several explainable AI (XAI) methods have been introduced to scrutinize the decision taken by the AI black box models. XAI methods generate the feature's contribution for any AI decision or prediction by calculating the attributions of every participated feature [8]. In other words, the primary purpose of XAI is to build a white-box model for providing information on the inner working of the AI models. Consequently, for any AI-enabled decisions, XAI helps to illustrate model fairness, accuracy, and transparency, which is required for any business/organization to provide confidence and trust when deploying AI models [9]. In particular, it is essential to include the XAI-monitored metrics [10] to assess

S. Roy and H. Chergui are with CTTC, Barcelona, Spain. C. Verikoukis is with University of Patras, Greece and Iquadrat Informatica, Spain. [e-mail: sroy@cttc.es, chergui@ieee.org, cveri@ceid.upatras.gr]

the trust level of various AI functions across the technological network domains or at the slice level for maintaining the SLA related to any services of the future AI-native 6G networks.

Moreover, AI transparency is particularly important for 6G zero-touch networks [8], [11]. Besides, the critical characteristic of 6G that is "human-centric" [11] rather than "machine-centric." This signifies that all the corresponding "smart things" in the 6G network will function intelligently for humans as a colossus but as a smart black box. In this respect, XAI plays a vital role in gaining the human's trust in the loop.

In a real deployment, however, the operator/slice tenant needs to understand the FL model's behavior at specific times (e.g busy hours) to trust it. Considering this fact, XAI empowered FL will be getting a particular focus for their end-user trust and secured operation.

A. Related Work

This section concentrates on XAI methods applied to the telecommunication domain. It is noteworthy that some previous papers [12], [13], [14] suggest expert knowledge like self-organizing map (SOM) and data clustering, Bayesian Network classifier, temporal analysis, etc., for providing explanations of the root cause issue of the violation in 5G networks. And such descriptions are beneficial to solve problems quickly. There are some domains like autonomous driving, image recognition, and speech analysis, to mention a few [15] where XAI methods have already gained popularity. Nevertheless, even now, in the telecommunication domain, it has not been explored that much. In this regard, the papers Differently, our work investigates the explanation directly generated from the training dataset—instead of using expert knowledge—and includes it as constraints for solving the optimization problems. Besides, there are numerous AI-based research works [16], [17], [18] for solving the issues related to resource allocation of 6G network slices. However, as far as our knowledge, most of them do not address the open problem of providing explainability in their proposed solutions.

The authors in [19] specify the challenges of developing XAI methods and show causal inference in 6G technology. The works [20], [21] emphasize the need for explainability of 5G to deliver critical services and for security aspects of device-to-device architecture in 5G networks, respectively. But all of this research work present only the importance of explainability in different telecommunication domains and network/application layers.

However, The authors of [22] mention the necessity for explainability in future 6G networks and provide a concise summary of applying XAI to solve handover and resource allocation problems. The paper of [7] presents a comparative analysis of the various XAI methods, like XGBoost, SHAP, PI, etc., in their model and concludes that SHAP is the best for finding the actual cause of the SLA violation. Nonetheless, they do not clearly explain the mismatch in their presented results, gathered from various gradient and permutation-based XAI methods, which makes the model reliability questionable. In [24] the authors describe the results of a network automation task by providing a human-understandable architecture.

Anyway, in the abovementioned works, no quantitative metrics are considered to evaluate the faithfulness of the explanations. Thus, to resolve that gap, the authors of [25] demonstrate an extensive range of XAI metrics for qualitative assessment of their proposed problem statement, ensuring trustworthiness. Here, they consider the SHAP method for explainability. However they neither tackle integration-based XAI methods nor show any comparative analysis of the various XAI methods, which is essential for getting more confidence about the behavior of their mentioned XAI methodology.

Meanwhile, In [8], the authors mention that the full automation of ZSM based framework depends on the interpretability and transparency of the AI/ML models to enhance trust and transparency for people to use 6G networks. In this context, one of the very recent works [26] proposes a neuro-symbolic XAI twin framework to promote the reasoning and trustworthiness of zero-touch Internet of Everything (IoE) service management in the wireless network. Even if they consider the extensibility and modularity of their work through logic and explainability, they do not consider a turbo-like explainable AI where explanation and AI model are iteratively included in a closed loop. Besides, the paper does not tackle distributed learning approach with XAI in the ZSM framework, which is essential for managing a massive number of coexisting and heterogeneous slices in the upcoming 6G networks under appropriate SLA requirements. On the other hand, the authors [27] present the concept of FL of XAI, mainly focusing on the importance of such an approach in 5G/6G networks. In comparison, quantitative validation of the faithfulness of the explanations is missing in their work. In [28] the authors apply a trust-aware deep reinforcement learning-based device selection technique using the Shapley Additive explanations (SHAP) method from XAI. Those devices later participate in an FL training process in an autonomous driving scenario.

Differently, in our work, we jointly integrate the SLA and Explainability-aware metrics as constraints in a turbo closed loop for optimizing slices' resource provisioning models in a 6G network, which is essential for actual deployment in live networks. We specifically use both gradient and perturbation XAI methods to generate the attributions for TEFL wherefore it maintains the performance superiority compared with a state-of-the-art integrated gradient post-hoc explained FL.

B. Contributions

In this paper, we present the following contributions

- We introduce a novel iterative explainable federated learning approach, where a constrained resource allocation model and an *explainer* exchange—in a closed loop way—soft attributions of the features as well as predictions to achieve a transparent and SLA-aware zero-touch service management of 6G network slices at RAN-Edge in a non-IID setup,
- We adopt the integrated gradients XAI method to showcase features attributions, and map them to the soft probability space,
- The soft attributions are then used to quantitatively validate the faithfulness of the explanations via the so-called *confidence metric* which is included as a constraint in the FL optimization task.
- We formulate the corresponding joint SLA and XAI-constrained optimization problem under the *proxy-Lagrangian* framework and solve it via a non-zero sum two-player game strategy, while comparing with the unconstrained integrated-gradient post-hoc FL baseline.
- We present a comparative analysis of additional XAI methods that are used to generate attributions for TEFL and assess their confidence metrics as well as explanation via correlation heatmaps.

C. Notations

We summarize the notations used throughout the paper in Table I.

TABLE I: Notations

Notation	Description
$S_\mu(\cdot)$	Logistic function with steepness μ
$F(\cdot)$	CDF
$\tilde{F}(\cdot)$	Complementary CDF
L	Number of local epochs
T	Number of FL rounds
$\mathcal{D}_{k,n}$	Dataset at CL (k,n)
$D_{k,n}$	Dataset size
$\ell(\cdot)$	Loss function
$\mathbf{W}_{k,n}^{(t)}$	Local weights of CL (k,n) at round t
$\mathbf{x}_{k,n}$	Input features
$\hat{x}_{k,n}^{(i,j)}$	Mutated features
$\hat{y}_{k,n}^{(i)}$	Allocated resource by CL (k,n)
α_n	Resource lower-bound for slice n
β_n	Resource upper-bound for slice n
γ_n	Threshold of CDF-based SLA for slice n
ν_n	Threshold of Confidence bound for slice n
$\mathcal{D}_{k,n}$	Samples whose prediction fulfills the SLA
$\hat{z}_{k,n}^{(i)}$	Predictions after mutation
$\pi_{k,n}^{(i,j)}$	Probability Distribution
$C_{k,n}$	Confidence Metric
$\alpha_{k,n}^{(i,j)}$	Weighted attribution of features
$\lambda_{(\cdot)}$	Lagrange multipliers
R_λ	Lagrange multiplier radius
$\mathcal{L}_{(\cdot)}$	Lagrangian with respect to $(\cdot)$

II. Network Architecture and Datasets

As depicted in Fig. 1, a 6G RAN-Edge topology under a per-slice central unit (CU)/distributed unit (DU) functional split has been considered, wherein DUs are co-located with the transmission/reception point (TRP), while each CU k is a virtual network function (VNF) running on top of a commodity hardware at the Edge domain and implements a closed loop (CL) $k\,(k = 1,\ldots,K)$ consisting of a key performance indicators (KPIs) collection as well as AI-enabled slice resource allocation functions. Specifically, the collected data serves to build local datasets for slice $n\,(n = 1,\ldots,n)$, i.e., $\mathcal{D}_{k,n} = \{\mathbf{x}_{k,n}^{(i)}, y_{k,n}^{(i)}\}_{i=1}^{D_{k,n}}$, where $\mathbf{x}_{k,n}^{(i)}$ stands for the input features vector while $y_{k,n}^{(i)}$ represents the corresponding output. In this respect, Table I summarizes the features and the output of the local datasets, which have been synthesized to mimic real hourly traffics of the main over-the-top (OTT) applications. These accumulated datasets are non-IID due to the different traffic profiles induced by the heterogeneous users' distribution and channel conditions. Moreover, since the collected datasets are generally non-exhaustive to train accurate resource allocation models, local CLs take part in a federated learning task wherein an E2E slice-level server plays the role of a model aggregator.

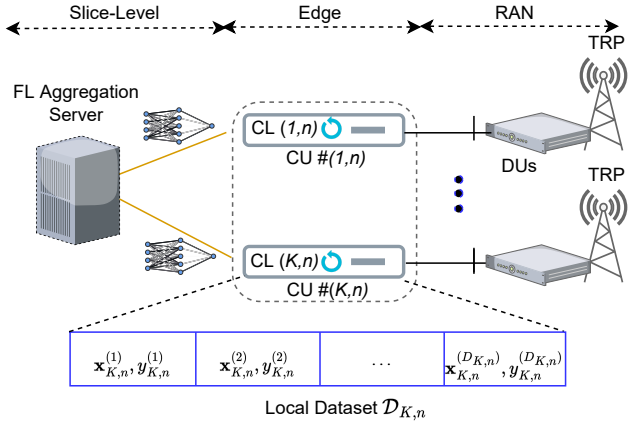

Fig. 1: Decentralized closed loops (CLs) architecture

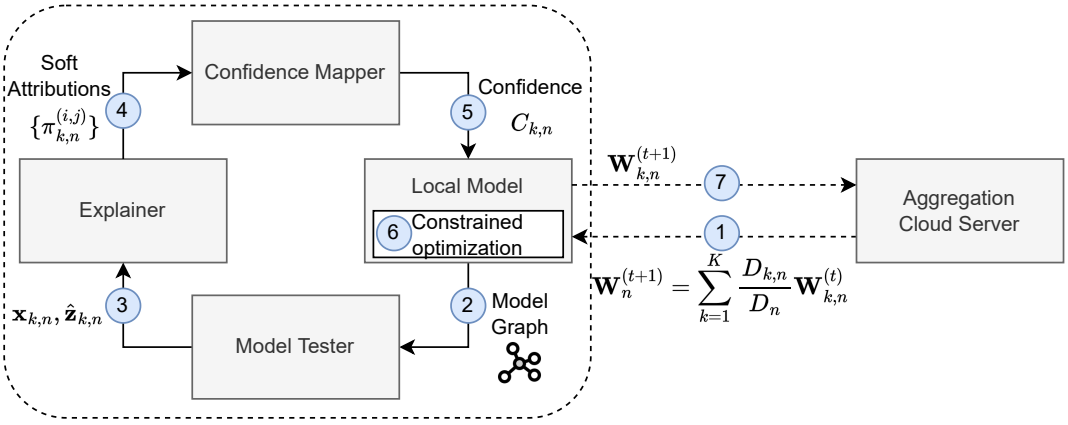

Fig. 2: Turbo explainable FL for transparent resource allocation

TABLE II: Dataset Features and Output

Feature	Description
`OTT Traffics`	Apple, Facebook, NetFlix, and Youtube etc.
`CQI`	Channel quality indicator
`S-MIMO Full-Rank`	Spatial MIMO full-rank usage (%)
`# Users`	Downlink Average active users

Output	Description
`CPU Load`	CPU resource consumption (%)

III. Turbo Explainable FL for Trustworthy Slice-level Resource Allocation

A. Concept

Inspired by the turbo principle, we propose a federated learning architecture where the local learning is performed iteratively with run-time explanation. For each local epoch, the Learner module feeds the posterior symbolic model graph to the Tester block which yields the test features and the corresponding predictions $z_{k,n}^{(i)}$ to the Explainer. The latter first generates the features attributions using one of the feature attribution XAI methods. It then converts these attributions to a soft probability distribution that is translated afterward into a confidence metric by the Confidence Mapper and fed back to the Learner to include it in the local constrained optimization as shown in Fig. 2.

Indeed, for each local CL (k, n), the predicted amount of resources $\hat{y}_{k,n}^{(i)}$, $(i = 1, \ldots, D_{k,n})$, should minimize the main loss function with respect to the ground truth $y_{k,n}^{(i)}$, while jointly respecting some long-term statistical constraints defined over its $D_{k,n}$ samples and jointly corresponding to SLA and explainability. As shown in steps 1 and 7 of Fig. 2, the optimized local weights at round t, $\mathbf{W}_{k,n}^{(t)}$, are sent to the server which generates a global FL model for slice n as,

$$\mathbf{W}_n^{(t+1)} = \sum_{k=1}^{K} \frac{D_{k,n}}{D_n} \mathbf{W}_{k,n}^{(t)}, \tag{1}$$

where $D_n = \sum_{k=1}^{K} D_{k,n}$ is the total data samples of all datasets related to slice n. The server then broadcasts the global model to all K CLs that use it to start the next round of turbo local optimization. Specifically, it leverages a two-player game strategy to jointly optimize over the objective and original constraints as well as their smoothed surrogates and detailed in the sequel.

B. Model Testing and Explanation

As depicted in stage 2 of Fig. 2, upon the reception of the updated model graph, the Tester uses a batch drawn from the local dataset to reconstruct the test predictions $\mathbf{z}_{k,n}^{(i)}$. All the graph, test dataset and the predictions are fed to the Explainer at stage 3 to generate the attributions, i.e., a quantified impact of each single feature on the predicted output. Let $\mathbf{a}_{k,n}^{(i)} \in \mathbb{R}^Q$ denote the attribution vector of sample i, which can be generated by any attribution-based XAI method. In our solution, we leverage the low-complexity Integrated Gradient (IG) scheme [29], which is based on the gradient variation when sampling the neighborhood of a feature. At stage 4, the Explainer then calculates what we call *soft attributions* by mapping the attributions into a probability space as follows,

$$\pi_{k,n}^{(i,j)} = \frac{\exp\left\{\left|\alpha_{k,n}^{(i,j)}\right|\right\}}{\sum_{q=1}^{Q} \exp\left\{\left|\alpha_{k,n}^{(i,q)}\right|\right\}}, \; j = 1, \ldots, Q, \tag{2}$$

where, $\alpha_{k,n}^{(i,j)} = a_{k,n}^{(i,j)} / x_{k,n}^{(i,j)}$ stands for the weighted attribution, since the sensitivity of the model's output with respect to an input feature in the neighborhood of the input is approximately

given by the ratio of the attribution for that input feature to the value of that feature [30].

C. Confidence Mapping

To characterize the trustworthiness of the local model, we invoke the confidence metric $C_{k,n}$ [31]. In this respect, the *Confidence Mapper* at stage 5 of Fig. 2 starts by performing a feature mutation, where it selects from the dataset feature $x_{k,n}^{(i,j)}$ with probability $\pi_{k,n}^{(i,j)}$, and changes it to the baseline value, i.e., zero,

$$\hat{x}_{k,n}^{(i,j)} = x_{k,n}^{(i,j)} \times (1-p),\ p \sim \mathcal{B}\left(1, \pi_{k,n}^{(i,j)}\right), \tag{3}$$

to force the change of the model's decision into the opposite category, In classification tasks, the categories (or subsets) are merely the classes. In our regression problem, we rather define the subsets in terms of SLA, that is,

$$\mathcal{D}_{k,n} = \mathcal{U}_{k,n} \cup \bar{\mathcal{U}}_{k,n}, \tag{4}$$

where $\mathcal{U}_{k,n}$ contains the samples whose prediction fulfills the SLA. The aforementioned transformation leads to a mutated dataset $\{\hat{x}_{k,n}^{(i,j)}\}$. The Confidence Mapper reports then the fraction of samples in the neighborhood for which the decision of the model,

$$\hat{z}_{k,n}^{(i)} = \mathcal{M}_{k,n}(\mathbf{W}_{k,n}^{(t)}, \hat{\mathbf{x}}_{k,n}^{(i)}), \tag{5}$$

does not move to the other set, that is, conforms to the original decision, as the conservatively estimated confidence measure [30], i.e.,

$$C_{k,n} = \frac{1}{u_{k,n}} \sum_{i=1}^{u_{k,n}} \max\left\{\mathbb{1}_{\mathbb{R}^-}\left(\alpha_n - \hat{z}_{k,n}^{(i)}\right), \mathbb{1}_{\mathbb{R}^-}\left(\hat{z}_{k,n}^{(i)} - \beta_n\right)\right\}, \tag{6}$$

where $\hat{z}_{k,n}^{(i)}$ are the predictions after mutation, while $u_{k,n}$ stands for the size of the considered original category $\mathcal{U}_{k,n}$.

D. Joint SLA and Explainability-Aware Resource Allocation

A long-term SLA states that the assigned resource to the tenant should not exceed a range $[\alpha_n, \beta_n]$ with a probability higher than an agreed threshold γ_n. Moreover, the confidence metric should be higher than a threshold ν_n. This translates to solving a statistically constrained local resource allocation problem as shown at stage 6, where both empirical cumulative density function (ECDF) and complementary ECDF (ECCDF) constraints at FL round $t\,(t = 0, \ldots, T-1)$ are involved, i.e.,

$$\min_{\mathbf{W}_{k,n}^{(t)}} \frac{1}{D_{k,n}} \sum_{i=1}^{D_{k,n}} \ell\left(y_{k,n}^{(i)}, \hat{y}_{k,n}^{(i)}\left(\mathbf{W}_{k,n}^{(t)}, \mathbf{x}_{k,n}\right)\right), \tag{7a}$$

$$\text{s.t. } F_{\mathbf{x}_{k,n}\sim\mathcal{D}_{k,n}}(\alpha_n) = \frac{1}{D_{k,n}} \sum_{i=1}^{D_{k,n}} \mathbb{1}_{\mathbb{R}^-}\left(\hat{y}_{k,n}^{(i)} - \alpha_n\right) \leq \gamma_n, \tag{7b}$$

$$\tilde{F}_{\mathbf{x}_{k,n}\sim\mathcal{D}_{k,n}}(\beta_n) = \frac{1}{D_{k,n}} \sum_{i=1}^{D_{k,n}} \mathbb{1}_{\mathbb{R}^-}\left(\beta_n - \hat{y}_{k,n}^{(i)}\right) \leq \gamma_n, \tag{7c}$$

$$C_{k,n} \geq \nu_n, \tag{7d}$$

which is solved by invoking the so-called *proxy Lagrangian* framework [**?**]. This consists first on considering two Lagrangians as follows:

$$\begin{aligned}\mathcal{L}_{\mathbf{W}_{k,n}^{(t)}} =& \frac{1}{D_{k,n}} \sum_{i=1}^{D_{k,n}} \ell\left(y_{k,n}^{(i)}, \hat{y}_{k,n}^{(i)}\left(\mathbf{W}_{k,n}^{(t)}, \mathbf{x}_{k,n}\right)\right) \\ &+ \lambda_1 \Psi_1\left(\mathbf{W}_{k,n}^{(t)}\right) + \lambda_2 \Psi_2\left(\mathbf{W}_{k,n}^{(t)}\right) \\ &+ \lambda_3 \Psi_3\left(\mathbf{W}_{k,n}^{(t)}\right),\end{aligned} \tag{8a}$$

$$\mathcal{L}_{\lambda} = \lambda_1 \Phi_1\left(\mathbf{W}_{k,n}^{(t)}\right) + \lambda_2 \Phi_2\left(\mathbf{W}_{k,n}^{(t)}\right) + \lambda_3 \Phi_3\left(\mathbf{W}_{k,n}^{(t)}\right) \tag{8b}$$

where $\Phi_{1,2,3}$ and $\Psi_{1,2,3}$ represent the original constraints and their smooth surrogates, respectively. Specifically, the indicator terms in (7b), (7c) and (7d) are replaced with Logistic functions and the soft maximum is used as surrogate of the maximum as,

$$\Psi_1\left(\mathbf{W}_{k,n}^{(t)}\right) = \frac{1}{D_{k,n}} \sum_{i=1}^{D_{k,n}} S_{\mu}\left(\alpha_n - \hat{y}_{k,n}^{(i)}\right) - \gamma_n \leq 0, \tag{9}$$

$$\Psi_2\left(\mathbf{W}_{k,n}^{(t)}\right) = \frac{1}{D_{k,n}} \sum_{i=1}^{D_{k,n}} S_{\mu}\left(\hat{y}_{k,n}^{(i)} - \beta_n\right) - \gamma_n \leq 0, \tag{10}$$

$$\begin{aligned}\Psi_3\left(\mathbf{W}_{k,n}^{(t)}\right) = \nu_n - \frac{1}{u_{k,n}} \sum_{i=1}^{u_{k,n}} \log\Big\{&\exp\left[S_{\mu}\left(\hat{z}_{k,n}^{(i)} - \alpha_n\right)\right] \\ &+ \exp\left[S_{\mu}\left(\beta_n - \hat{z}_{k,n}^{(i)}\right)\right]\Big\} \leq 0,\end{aligned} \tag{11}$$

where L_{μ} stands for the Logistic function with steepness parameter μ, i.e.,

$$S_{\mu}(\theta) = \frac{1}{1 + e^{-\mu\theta}}. \tag{12}$$

This optimization task turns out to be a non-zero-sum two-player game in which the $\mathbf{W}_{k,n}^{(t)}$-player aims at minimizing $\mathcal{L}_{\mathbf{W}_{k,n}^{(t)}}$, while the λ-player wishes to maximize $\mathcal{L}_{\lambda}$ [**?**, Lemma 8]. While optimizing the first Lagrangian w.r.t. $\mathbf{W}_{k,n}$ requires differentiating the constraint functions $\Psi_1(\mathbf{W}_{k,n}^{(t)})$, $\Psi_2(\mathbf{W}_{k,n}^{(t)})$ and $\Psi_3(\mathbf{W}_{k,n}^{(t)})$, to differentiate the second Lagrangian w.r.t. λ we only need to evaluate $\Phi_1\left(\mathbf{W}_{k,n}^{(t)}\right)$, $\Phi_2\left(\mathbf{W}_{k,n}^{(t)}\right)$ and $\Phi_3\left(\mathbf{W}_{k,n}^{(t)}\right)$. Hence, a surrogate is only necessary for the

$\mathbf{W}_{k,n}$-player; the λ-player can continue using the original constraint functions. The local optimization task can be written as,

$$\min_{\mathbf{W}_{k,n}\in\Delta} \quad \max_{\lambda,\,\|\lambda\|\leq R_\lambda} \quad \mathcal{L}_{\mathbf{W}_{k,n}^{(t)}} \tag{13a}$$

$$\max_{\lambda,\,\|\lambda\|\leq R_\lambda} \quad \min_{\mathbf{W}_{k,n}\in\Delta} \mathcal{L}_\lambda, \tag{13b}$$

where thanks to Lagrange multipliers, the λ-player chooses how much to weigh the proxy constraint functions, but does so in such a way as to satisfy the original constraints, and ends up reaching a nearly-optimal nearly-feasible solution [33]. These steps are all summarized in Algorithm 1.

Algorithm 1: Turbo Explainable Federated Learning

Input: K, m, η_λ, T, L. `# See Table III`
Server initializes $\mathbf{W}_n^{(0)}$ and broadcasts it to the CLs
for $t = 0, \ldots, T-1$ **do**
  parallel for $k = 1, \ldots, K$ **do**
  Initialize $M =$ `num_constraints` and $\mathbf{W}_{k,n,0} = \mathbf{W}_n^{(t)}$
  Initialize $\mathbf{A}^{(0)} \in \mathbb{R}^{(M+1)\times(M+1)}$ with $\mathbf{A}^{(0)}_{m',m} = 1/(M+1)$
  for $l = 0, \ldots, L-1$ **do**
    Receive the graph $\mathcal{M}_{k,n}$ from the local model
    `# Test the local model and calculate the attributions`
    $a_{k,n}^{i,j} =$ `Int. Gradient` $\left(\mathcal{M}_{k,n}\left(\mathbf{W}_{k,n,l}, \mathbf{x}_{k,n}\right)\right)$
    `# Generate soft attributions`
    $\pi_{k,n}^{(i,j)} = \frac{\exp\left\{\left|\alpha_{k,n}^{(i,j)}\right|\right\}}{\sum_{p=1}^{L}\exp\left\{\left|\alpha_{k,n}^{(i,p)}\right|\right\}}$, $j = 1, \ldots, Q$,
    `# Mutate the test dataset`
    Mutate $x_{k,n}^{(i,j)}$ with probability $\pi_{k,n}^{(i,j)}$
    `# Calculate the confidence metric`
    $C_{k,n} = \frac{\sum_{i=1}^{u_{k,n}} \max\left\{\mathbb{1}_{\mathbb{R}^-}\left(\alpha_n - \hat{z}_{k,n}^{(i)}\right), \mathbb{1}_{\mathbb{R}^-}\left(\hat{z}_{k,n}^{(i)} - \beta_n\right)\right\}}{u_{k,n}}$
    Let $\lambda^{(l)}$ be the top eigenvector of $\mathbf{A}^{(l)}$
    `# Solve problem (7) via oracle optimization`
    Let $\hat{\mathbf{W}}_{k,n,l} = \mathcal{O}_\delta\left(\mathcal{L}_{\mathbf{W}_{k,n,l}}(\cdot, \hat{\lambda}^{(l)})\right)$
    Let $\Delta_\lambda^{(l)}$ be a gradient of $\mathcal{L}_\lambda(\hat{\mathbf{W}}_{k,n,l}, \lambda^{(l)})$ w.r.t. λ
    `# Exponentiated gradient ascent`
    Update $\tilde{\mathbf{A}}^{(l+1)} = \mathbf{A}^{(l)} \odot \cdot \exp\left\{\eta_\lambda \Delta_\lambda^{(l)}(\lambda^{(l)})\right\}$
    `# Colunm-wise normalization`
    $\mathbf{A}_m^{(l+1)} = \tilde{\mathbf{A}}_m^{(l+1)} / \left\|\mathbf{A}_m^{(l+1)}\right\|_1$, $m = 1, \ldots, M+1$
  end
  return $\hat{\mathbf{W}}_{k,n}^{(t)} = \frac{1}{L^\star}\sum_{l=0}^{L-1}\hat{\mathbf{W}}_{k,n,l}$
  Each local CL (k,n) sends $\hat{\mathbf{W}}_{k,n}^{(t)}$ to the server.
  end parallel for
  return $\mathbf{W}_n^{(t+1)} = \sum_{k=1}^{K}\frac{D_{k,n}}{D_n}\hat{\mathbf{W}}_{k,n}^{(t)}$
  and broadcasts the value to all local CLs.
end

IV. Results

In this section we evaluate the proposed TEFL framework by first justifying the use of feature attributions as a pillar to build the explainability-aware constrained resource allocation model. We then present the FL convergence, confidence score and SLA fulfilment performance and showcase their underlying trade-offs. Finally, we study the correlation between features attributions and SLA violation and draw some important conclusions. Specifically, to implement the model Tester and Explainer, we invoke `DeepExplain` framework, which includes state-of-the-art gradient and perturbation-based attribution methods [34]. It provides an attribution score based on the feature's contribution to the model's output, which we integrate with our proposed constrained resource allocation FL framework in a closed-loop iterative way.

A. Parameter Settings and Baseline

We consider below three primary slices to analyze the proposed Explainable FL policy, defined as follows:

- **eMBB:** Netflix, Youtube and Facebook Video,
- **Social Media:** Facebook, Facebook Messages, Whatsapp and Instagram,
- **Browsing:** Apple, HTTP and QUIC,

Here, the traffic associated with each mentioned slice is the sum of the underlying OTTs' traffics that collects from the hourly traffics of the slices for five days, and the overall summary of those datasets are presented in Table II at section II. We use vectors α, β for the resource bounds,γ for the thresholds corresponding to the different slices for a particular resource and ν for explainable metrics threshold .The parameters settings are mentioned in Table III.

TABLE III: Settings

Parameter	Description	Value
N	# Slices	3
K	# CLs	100
$D_{k,n}$	Local dataset size	1000 samples
T	# Max FL rounds	30
L	# Local epochs	100
R_λ	Lagrange multiplier radius	Constrained: 10^{-5}
η_λ	Learning rate	0.02

B. Rationale behind the Confidence Metric

Here, we describe the motivation for preferring attribution-based confidence metric. As previously mentioned, sampling over the surrounding high-magnitude inputs is an acceptable way to determine the model's conformance. Such an approach is vital because there will likely be no change in the label if we do sampling over low attribution features space. Also, it indicates that the model is similar in these features. Furthermore, it is noteworthy that deep learning models reveal an engagement of features. So, in our proposed method, we consider high-magnitude input spaces to estimate the confidence score by focusing on high attribution feature space during sampling. Following the above approach, we have

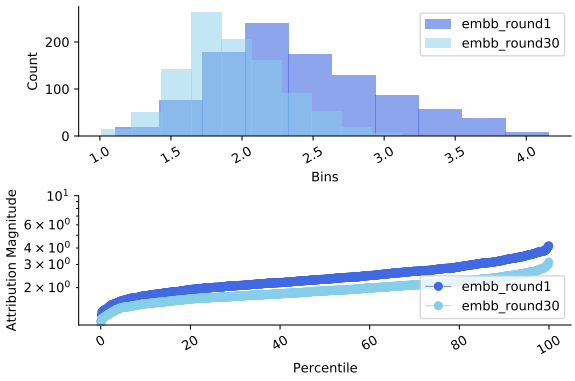

(a) Attribution Magnitude for Constrained TEFL Embb Slice

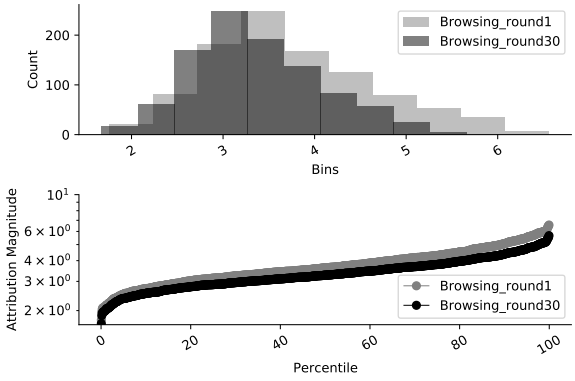

(b) Attribution Magnitude for Constrained TEFL Browsing Slice

Fig. 3: Attribution SLA resource bound with $\alpha = [0, 0, 0]$, $\beta = [4, 6, 8]$, $\gamma = [0.01, 0.01, 0.01]$ and $\nu = [0.9, 0.8, 0.85]$

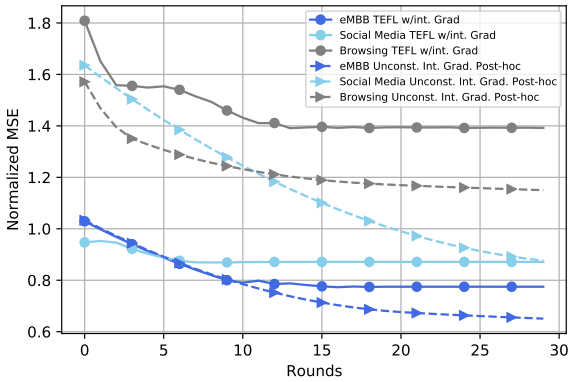

Fig. 4: FL training MSE loss vs. FL rounds of proposed TEFL with SLA resource bound, $\alpha = [0, 0, 0]$, $\beta = [4, 6, 8]$, $\gamma = [0.01, 0.01, 0.01]$ and $\nu = [0.9, 0.8, 0.85]$

plotted the attribution magnitude vs. percentile of and have provided attributions' histograms in the case of TEFL as shown in Fig. 3. Here, we consider eMBB and Browsing slices to demonstrate the above theoretical approach. From the histogram graph, we can visualize the distribution of the attribution score datasets. In contrast, the percentile graph gives us more insights into the percentage of attribution scores that fall below a particular value which is the mean value of the distribution in our case. Moreover, we can quickly get the approximate mean data point from the histogram plot. So, at the mean data point, the approximate percentile score for both slices is around 42 %, which means around 60 % of features have high attribution scores. This analysis directs us to focus on the high magnitude input space for computing the confidence matrix. Furthermore, We can also observe that the model keeps the same normal distribution pattern from the beginning to the end of the overall training round. According to the Central limit theorem, such characteristics are essential for ML model building and mathematical convenience. So this intuition motivates us to go forward.

C. Result Analysis

In this scenario, resources at CU-level are dynamically allocated to slices according to their traffic patterns and radio conditions (average CQI, MIMO full-rank usage) while ensuring a long term isolation via the constrains imposed to the underlying resources.

- **Convergence and SLA:** As depicted in Fig. 4 and Fig. 5, we can conclude that the proposed constrained TEFL resource allocation model of the different slices has converged faster with significantly lower violation rates than the baseline unconstrained IG post-hoc case. Precisely, the SLA violation rate of the proposed one is in close proximity to the target threshold γ (i.e., around

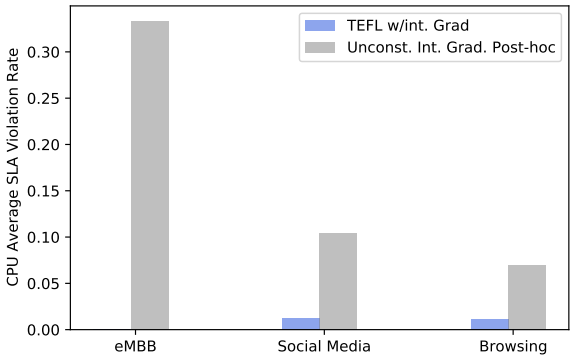

Fig. 5: SLA violation rate of TEFL $\alpha = [0, 0, 0]$, $\beta = [4, 6, 8]$, $\gamma = [0.01, 0.01, 0.01]$ and $\nu = [0.9, 0.8, 0.85]$

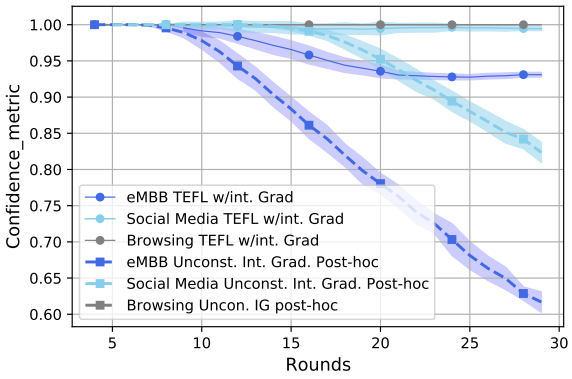

(a) Model confidence metric vs. number of FL rounds

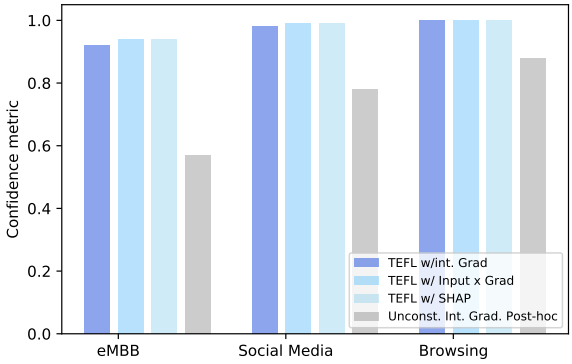

(b) Confidence metric with TEFL on test dataset

Fig. 6: Analysis of different XAI methods with $\alpha = [0, 0, 0]$, $\beta = [4, 6, 8]$, $\gamma = [0.01, 0.01, 0.01]$ and $\nu = [0.9, 0.8, 0.85]$

1%), which is an acceptable value for operators and slices' tenants.

- **Trustfulness:** To evaluate the proposed algorithm's performance and trustworthiness, we have plotted the model confidence metric vs. the FL rounds in Fig. 6-(a), considering TEFL and the baseline unconstrained IG post-hoc. In this respect we notice again that the statistics of the XAI-based confidence metric give us an approximate idea of our model's reliability. It shows that the confidence metric of the proposed one for all different slices has a higher value above 90% in the constrained TEFL case, which conveys that our model is explainable and also trustable in the training phase. Besides, the Explainer block in Fig. 2 is also implemented using both perturbation-based XAI method SHAP and gradient-based method Input*Gradient [35], where Fig. 6-(b) confirms that our proposed TEFL algorithm preserves the same behavior during the testing phase. Moreover, the confidence score has remained almost the same even if the attribution scores have been generated by various XAI methods, which makes our proposed algorithm more reliable.

Overall, based on the presented results in Fig. 6, we remark that the lower confidence value of the model induces a higher SLA violation rate and vice versa. Apart from this, the constrained TEFL ensures a trade-off between convergence and confidence, i.e., model confidence is decreased with the decreasing loss within an allowable confidence threshold. Ultimately, we achieve desired behavior of our model by the proposed approach with the confirmation of the model's trustworthiness.

Furthermore, we demonstrate in Fig. 7 the correlation heatmaps of the proposed XAI method with other XAI techniques and consider only the social media slice for further analysis. This approach helps us visualize the strength of relationships between different variables and, in our case, identify which feature variation impacts the most for SLA variation. To plot correlation matrix heatmap, we consider one matrix, $\mathbf{R}_{k,n} = [\mathbf{a}_{k,n}, \hat{\mathbf{z}}_{k,n}, \mathbf{s}_{k,n}]$, where, $\mathbf{a}_{k,n}$ is the attribution score of features variable with dimensions $D_{k,n} \times Q$ and $\hat{\mathbf{z}}_{k,n}$

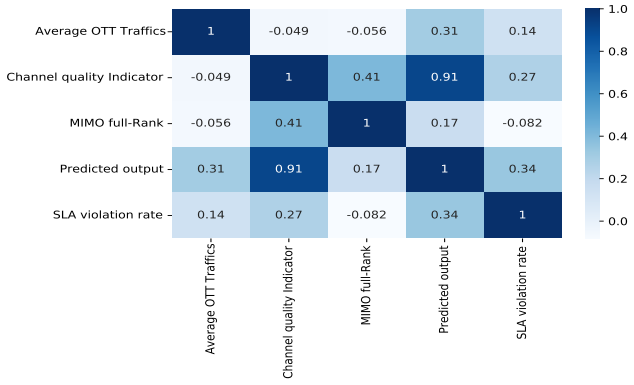

(a) TEFL w/ Int. Grad.

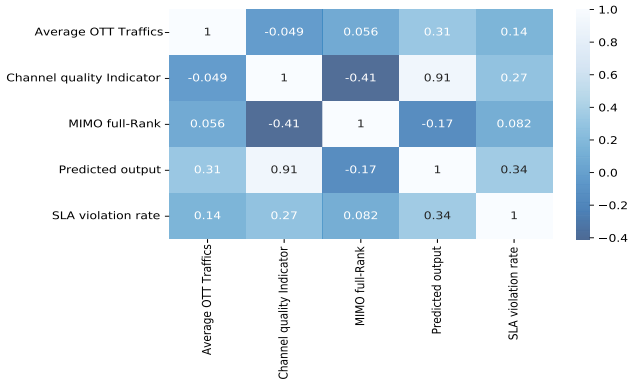

(b) TEFL w/ Input x Grad. (extension of Saliancy)

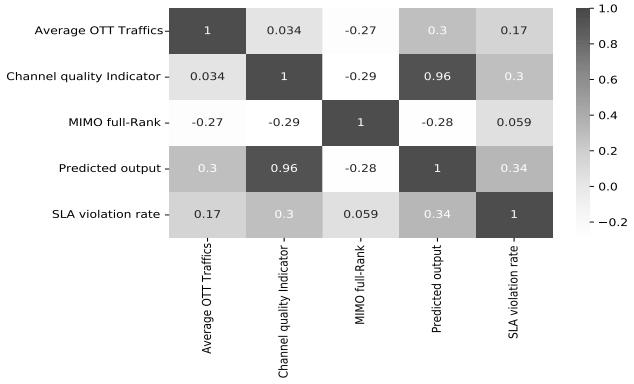

(c) TEFL w/ SHAP

Fig. 7: Correlation heatmap of social media slice for three different XAI methods

is the predicted output variable with dimensions $D_{k,n} \times 1$ and $\mathbf{s}_{k,n}$ is the binary representation of the SLA variation with dimensions $D_{k,n} \times 1$. From the heatmap we see that the second feature, which is the channel quality indicator, has the most impact on the SLA variation. If the second feature increases, the SLA variation will increase and vice versa. Notice that, in all applied XAI methods in Fig. 7, we get quite similar results for the importance of feature predictions. This comparative analysis gives us confidence about the proposed algorithm and show that it is generalizable.

V. Conclusion

In this paper, we have presented a novel iterative explainable federated learning (FL) approach to achieve a transparent and SLA-aware zero-touch service management (ZSM) of 6G network slices. We have considered SLA and XAI-based confidence metric jointly and in a closed loop way to solve the underlying optimization task using a proxy-Lagrangian two-player game strategy. In particular, we have used various XAI schemes to generate the attributions consumed by TEFL that presents the same superior performance compared to an unconstrained IG post-hoc FL baseline.

Eventually, at the end of the paperwork, we have shown the heat maps of the correlation matrix. So considering the analytic results of heatmaps, in the future, we can plan to work on the interpretation of the feature analysis of any dataset as well as give more importance to some specific feature sets to avoid SLA violation, and consider a more meaningful complex topology.

VI. Acknowledgment

This work has been supported in part by the training and research project SEMANTIC (861165), and 5G-ERA project (101016681).

References

[1] Z. Yan, J. Ge, Y. Wu, L. Li and T. Li, "Automatic Virtual Network Embedding: A Deep Reinforcement Learning Approach With Graph Convolutional Networks," in *IEEE Journal on Selected Areas in Communications,* vol. 38, no. 6, pp. 1040-1057, June 2020, doi: 10.1109/JSAC.2020.2986662.

[2] ETSI GS ZSM 002, "Zero-touch network and Service Management (ZSM); Reference Architecture," Aug. 2019.

[3] Brik, B. and Ksentini, A., 2020, November. On Predicting Service-oriented Network Slices Performances in 5G: A Federated Learning Approach. In 2020 *IEEE 45th Conference on Local Computer Networks (LCN)* (pp. 164-171). IEEE.

[4] H. Elayan, M. Aloqaily, and M. Guizani, "Internet of Behavior (IoB) and Explainable AI Systems for Influencing IoT Behavior," *CoRR,* vol. abs/2109.07239, 2021; https://arxiv.org/ abs/2109. 07239

[5] Rudin, Cynthia. "Stop explaining black box machine learning models for high stakes decisions and use interpretable models instead." *Nature Machine Intelligence 1.5* (2019): 206-215.

[6] M. Asif Habibi et al., "The Structure of Service Level Agreement of Slice-Based 5G Network" (Invited Paper), in the *29th Annual IEEE International Symposium on Personal, Indoor and Mobile Radio Communications (PIMRC)*, Bologna, Italy, September 2018.

[7] A. Terra, R. Inam, S. Baskaran, P. Batista, I. Burdick and E. Fersman, "Explainability Methods for Identifying Root-Cause of SLA Violation Prediction in 5G Network," *GLOBECOM 2020 - 2020 IEEE Global Communications Conference*, 2020, pp. 1-7, doi: 10.1109/GLOBECOM42002.2020.9322496.

[8] Wang, Shen, et al. "Explainable AI for B5G/6G: Technical Aspects, Use Cases, and Research Challenges." *arXiv preprint* arXiv:2112.04698 (2021).

[9] Belle, Vaishak, and Ioannis Papantonis. "Principles and practice of explainable machine learning." *Frontiers in big Data* (2021): 39.

[10] Hoffman, Robert R. et al. "Metrics for Explainable AI: Challenges and Prospects." *ArXiv* abs/1812.04608 (2018): n. pag.

[11] C. Benzaid and T. Taleb, "AI-Driven Zero Touch Network and Service Management in 5G and Beyond: Challenges and Research Directions," in *IEEE Network*, vol. 34, no. 2, pp. 186-194, March/April 2020, doi: 10.1109/MNET.001.1900252.

[12] A. Gomez-Andrades, P. Munoz, I. Serrano and R. Barco, "Automatic Root Cause Analysis for LTE Networks Based on Unsupervised Techniques," in *IEEE Transactions on Vehicular Technology*, vol. 65, no. 4, pp. 2369-2386, April 2016, doi: 10.1109/TVT.2015.2431742.

[13] H. Mfula and J. K. Nurminen, "Adaptive root cause analysis for self-healing in 5G networks," in *Conference on High Performance Computing Simulation*, 2017.

[14] P. Munoz, I. de la Bandera, E. J. Khatib, A. Gomez-Andrades, I. Serrano and R. Barco, "Root Cause Analysis Based on Temporal Analysis of Metrics Toward Self-Organizing 5G Networks," in *IEEE Transactions on Vehicular Technology,* vol. 66, no. 3, pp. 2811-2824, March 2017, doi: 10.1109/TVT.2016.2586143

[15] Dosilovic, Filip Karlo et al. "Explainable artificial intelligence: A survey." 2018 41st *International Convention on Information and Communication Technology, Electronics and Microelectronics (MIPRO)* (2018): 0210-0215.

[16] F. Fossati, S. Moretti and S. Secci, "Multi-resource allocation for network slicing under service level agreements", *Proc. 10th Int. Conf. Netw. Future (NoF),* pp. 48-53, Oct. 2019.

[17] Y. Li, A. Huang, Y. Xiao, X. Ge, S. Sun and H.-C. Chao, "Federated orchestration for network slicing of bandwidth and computational resource", arXiv:2002.02451, 2020, [online] Available: http://arxiv.org/abs/2002.02451.

[18] H. Chergui, L. Blanco and C. Verikoukis, "Statistical Federated Learning for Beyond 5G SLA-Constrained RAN Slicing," in *IEEE Transactions on Wireless Communications*, vol. 21, no. 3, pp. 2066-2076, March 2022, doi: 10.1109/TWC.2021.3109377.

[19] Y. Xiao, G. Shi, and M. Krunz, "Towards ubiquitous AI in 6G with federated learning," in *IEEE Communication Magazine*, 2020.

[20] Challita, Ursula & Ryden, Henrik & Tullberg, Hugo. (2020). When Machine Learning Meets Wireless Cellular Networks: Deployment, Challenges, and Applications. *IEEE Communications Magazine.* 58. 12-18. 10.1109/MCOM.001.1900664.

[21] A. Vijay and K. Umadevi, "Secured AI guided architecture for D2D systems of massive MIMO deployed in 5G networks," in *(ICOEI)*, 2019.

[22] C. Li, W. Guo, S. C. Sun, S. Al-Rubaye and A. Tsourdos, "Trustworthy Deep Learning in 6G-Enabled Mass Autonomy: From Concept to Quality-of-Trust Key Performance Indicators," in *IEEE Vehicular Technology Magazine*, vol. 15, no. 4, pp. 112-121, Dec. 2020, doi: 10.1109/MVT.2020.3017181.

[23] Lundberg, Scott M., and Su-In Lee. "A unified approach to interpreting model predictions." Advances in neural information processing systems 30 (2017).

[24] Y. Wu, G. Lin and J. Ge, "Knowledge-Powered Explainable Artificial Intelligence for Network Automation toward 6G," in IEEE Network, vol. 36, no. 3, pp. 16-23, May/June 2022, doi: 10.1109/MNET.005.2100541.

[25] Barnard, Pieter; Macaluso, Irene; Marchetti, Nicola; Pereira da Silva, Luiz (2021): Resource Reservation in Sliced Networks: An Explainable Artificial Intelligence (XAI) Approach. *TechRxiv. Preprint.* https://doi.org/10.36227/techrxiv.16702798.v1

[26] Munir, Md, et al. "Neuro-symbolic Explainable Artificial Intelligence Twin for Zero-touch IoE in Wireless Network." arXiv preprint arXiv:2210.06649 (2022).

[27] Renda, A.; Ducange, P.; Marcelloni, F.; Sabella, D.; Filippou, M.C.; Nardini, G.; Stea, G.; Virdis, A.; Micheli, D.; Rapone, D.; Baltar, L.G. Federated Learning of Explainable AI Models in 6G Systems: Towards Secure and Automated Vehicle Networking. Information 2022, 13, 395. https://doi.org/10.3390/info13080395

[28] G. Rjoub, J. Bentahar and O. A. Wahab, "Explainable AI-based Federated Deep Reinforcement Learning for Trusted Autonomous Driving," 2022 *International Wireless Communications and Mobile Computing (IWCMC)*, 2022, pp. 318-323, doi: 10.1109/IWCMC55113.2022.9824617.

[29] Mukund Sundararajan, Ankur Taly, and Qiqi Yan. 2017. Axiomatic attribution for deep networks. *In Proceedings of the 34th International Conference on Machine Learning* - Volume 70 (ICML'17). JMLR.org, 3319–3328.

[30] S. Jha, *et. al.,* "Attribution-based confidence metric for deep neural networks," in *Proceedings of the 33rd International Conference on Neural Information Processing Systems,* NY, USA, 2019..

[31] Jha, Susmit et al. "Attribution-Based Confidence Metric For Deep Neural Networks." NeurIPS (2019).

[32] https://github.com/marcoancona/DeepExplain

[33] G. J. Gordon, A. Greenwald, and C. Marks, "No-regret learning in convex games," in *ICML'08,* pp. 360-367, 2008.

[34] https://github.com/marcoancona/DeepExplain

[35] Kakogeorgiou, Ioannis, and Konstantinos Karantzalos. "Evaluating explainable artificial intelligence methods for multi-label deep learning classification tasks in remote sensing." International Journal of Applied Earth Observation and Geoinformation 103 (2021): 102520.